Distortion of atomic states by time-dependent electric fields

Predrag Krstić and Yukap Hahn
Physics Department, University of Connecticut, Storrs, Connecticut 06269
(Received 19 March 1993)

A class of approximate solutions of the Schrödinger equation for an atom in a time-dependent electric field that scales with the applied field F as $\int F(t)dt$ is derived and their bounds of validity are carefully examined. The class covers a wide region of applicable electric fields and its time constants. An extensive comparison of these solutions with the results of numerical calculations on a truncated basis of up to 465 hydrogenic states shows surprising agreement. One of these solutions is found to be very effective in field dressing of high Rydberg states. The resulting field dressing is proposed for the description of the plasma field effects on atomic reaction rates, but its range of applicability can be extended to the other atomic problems that involve time-dependent electric fields.

PACS number(s): 32.60.+i, 31.70.Hq

I. INTRODUCTION

The need for accurate evaluation of atomic reaction rates which are used in plasma modeling and diagnostics of high-temperature fusion plasmas and in astrophysical applications has attracted much effort in recent years [1–3]. However, external and intrinsic electric (and/or magnetic) fields [4,5] can sometimes drastically affect the rates. The collisional transitions of the atomic system caused by the plasma particles can also be sizable [6–12] at the densities of interest to fusion plasmas. This problem is especially critical for the high Rydberg states (HRS), where the high density of the levels with high degeneracy makes the plasma field effect (PFE) difficult to treat in general.

The PFE's consist of a stochastic perturbation of the atomic system by plasma electrons and ions that includes both the field distortion of the atomic states and collisional transitions caused by the plasma particles. The main task in the formulation of the PFE theory is to reduce the explicit dependence of the system on the plasma perturbers in a consistent manner by appropriate statistical averaging of the perturbations. This can be done by deriving a set of effective plasma potentials (EPP). This problem was treated elsewhere [8], where it was shown that within the range of the plasma concentrations of interest, the effective plasma potential in its crudest version may be expressed as an effective dipole electric field

$$V_p = \frac{\mathbf{r}\cdot\mathbf{R}_p}{R_p^3} , \tag{1.1}$$

where the time-dependent R_p depends on the concentration-dependent impact parameter b and the temperature-dependent plasma particle velocity v. V_p varies on the time scale b/v, with the electric field amplitude $1/b^2$. (Atomic units will be used throughout the text.) Once the effective Hamiltonians that contain the EPP are derived, the collisional transitions can be studied by deriving the various rates using the field-distorted wave functions.

The influence of the plasma environment on individual atomic states has been treated in the past by two seemingly distinct approaches: (a) The pressure-broadening theory (PBT) of spectral lines [6,7,9,10] that treated the electronic and ionic perturbations, usually in the lowest nonvanishing order, and (b) the rate equation (REQ) approach [11,12] that emphasized the collisional transition effect but neglected the field distortion problem. Recent studies (Refs. [13,14], and references therein) of the time-dependent Stark effect have contributed to further development of the PBT of the low-lying states, including nonperturbative methods and numerical simulations. However, for the situations that are of interest to the present problem involving HRS, the PFE's are highly nonperturbative, and the distortion of the wave functions has to be carefully evaluated. On the other hand, the complex, multistep transitions caused by the plasma particles are often treated by solving an approximate set of rate equations that contains a number of excited Rydberg states, which may be severely affected by the plasma fields. But the field mixing of the atomic states has not been included either in the rate calculations or in the rate equations.

Even if the EPP's are available [8], the inclusion of PFE's in the above treatments poses a formidable numerical task. Therefore simple field-dressed atomic wave functions that describe the system including the HRS as accurately as possible, with the known bounds of validity, are of importance for improvement of the description of PFE's. Theoretical description of such dressing by a time-dependent electric field is the main purpose of this work.

The problem of a hydrogen atom in a static electric field is well understood [15,16]. The Schrödinger equation in parabolic coordinates is separable, and the problem is reduced to solving two second-order ordinary differential equations, linked by the separation constants. Even then, there are serious technical difficulties in quantum treatment of the problem, due to substantial mixing of the continuum in the case of strong electric field, or to the large-order perturbation theory needed to describe the processes involving highly excited atomic states. One

possible approach to the problem, the WKB theory, was extensively exploited for atoms in static fields [17,18].

When the time dependence of the field is encountered, as it is in the case of our interest, the Schrödinger equation is no longer separable, and some nonperturbative methods or time-dependent perturbation theory to high orders must be employed. Furthermore, the finite time the atom is embedded in the field can introduce simplifications in the treatment. If that time is short enough, or if the field is weak enough, the presence of the continuum components in the bound states may be greatly reduced. The time constant of the field therefore represents an additional parameter to control the magnitude of the field-induced mixing of the states, and in many physical situations of interest its value can introduce significant limitations on the evolution of the system in the electric field. Our approach is to approximately sum the full time-dependent perturbation series of the problem and study their bounds of validity.

The time dependence of the field is assumed in its basic form

$$\mathbf{F}=F_0\exp(-\gamma|t|)\hat{\mathbf{e}} \ . \tag{1.2}$$

The exact solutions of the problem can be found in the limits $\gamma\rightarrow\infty$ and $\gamma\rightarrow 0$, with corresponding limitation on the classical velocity amplitude of the electron in the electric field, $g_0=F_0/\gamma$; in both limits, g_0 must be kept finite. It is the classical velocity of the perturber electron (or ion),

$$\mathbf{g}=\int \mathbf{F}(t)dt \ , \tag{1.3}$$

that is present as the only field-dependent parameters in the solutions. Therefore we define a class of solutions of the Schrödinger equation for the electron in a time-dependent electric field that scales with g. The general condition $\gamma\rightarrow\infty$ is read as $\gamma\gg 1/T$, where T is the characteristic time of the corresponding electron orbit, while $\gamma\rightarrow 0$ corresponds to $\gamma\ll 1/T$. Obviously, the former is easily satisfied for the HRS, while the latter is limited to the low-lying states. The condition of applicability is also tied to the electric field amplitude, limiting its values from above. These are derived and discussed in Sec. II. The major part of this work is the extensive numerical check on the validity of the formulas derived in Sec. II. This is carried out in Sec. III by solving various sets of time-dependent coupled differential equations constructed with truncated bases of hydrogenic states up to $n=30$ (with fixed magnetic quantum number m), and varying the field parameters. Although both in Sec. II and in Sec. III calculations are defined as an initial-value problem and tested for initially populated states up to $n=20$, the basis set for the numerical calculations is purposely oversized in order to simulate the continuum by the Rydberg states that are well above a chosen initial state. The derived formulas are valid for arbitrary direction of the electric field, with the time constants $1/\gamma$ not necessarily equal in different directions (the situation present in plasma dipole field). When the quantum number m is not conserved, numerical checks are performed also with the basis set of hydrogenic states below $n=10$. These numerical calculations, to which we will refer in this text as "exact," show a surprisingly good agreement with the approximate formulas within the defined bounds of validity, thus supporting the applicability of the approximate formulas to the EPP. Our discussion and conclusions are presented in Sec. IV.

We note that the assumed exponential time dependence of the field is not critical for the validity of the approximation. In particular, also successfully tested are the dipole perturber time dependence along the straight-line trajectory, a Gaussian time dependence, and oscillating nonresonant electric field with exponential switching conditions [19,20]. With slight adjustments of the field amplitude F_0 and time constant $1/\gamma$ in Eq. (1.2), the bounds of validity discussed in Secs. II and III can also be applied to these cases.

The main results of this paper on the validity of the approximations developed in Sec. II are summarized in Sec. IV.

II. THEORY AND ITS BOUNDS OF VALIDITY

Our starting point for derivation of simple approximations to distortion of electronic wave function under the influence of central potential $V(r)$ and time-dependent electric field $\mathbf{F}(t)$ is the time-dependent Schrödinger equation

$$\left[i\frac{\partial}{\partial t}-H\right]\Psi=0 \ , \tag{2.1a}$$

$$H=H_A+V_p \ , \tag{2.1b}$$

$$V_p=-\mathbf{r}\cdot\mathbf{F}(t) \ , \tag{2.1c}$$

where H_A is the atomic Hamiltonian ($\hbar=m=e^2=1$)

$$H_A=-\frac{\Delta}{2}+V(r) \ , \tag{2.2a}$$

whose eigenfunctions are defined by the equation

$$\left[i\frac{\partial}{\partial t}-H_A\right]\Phi_\nu=0 \ . \tag{2.2b}$$

In the case of the hydrogenic atom

$$V=-\frac{Z}{r} \ . \tag{2.2c}$$

The problem could be defined as an initial-value problem, with initial condition $\Psi(-\infty)=\Phi_0$, where index 0 means a set of spherical quantum numbers (n_0,l_0,m_0). Without loss of generality and for the purpose of the present section, the electric field is defined by exponential time dependence, Eq. (1.2), and is directed along the z axis. As will be discussed later in this section this can be generalized such that the field can take an arbitrary instantaneous direction to the fixed coordinate system, with two or more components of the form (1.2) where the γ's and F_0's for the different directions need not be the same.

In the following, all expansion parameters P and p are such that the convergence of perturbation series is ensured by P (or p) <1.

A. "Short-pulse" approximation

One can define Ψ in terms of an exact perturbation series in V_p, with $\mathbf{F}$ defined by Eq. (1.2), which for $t\leq 0$ takes the form

$$\Psi=\Phi_0+\sum_{j=1}^{\infty}\left[\sum_{\nu_1}\cdots\sum_{\nu_j}\Phi_{\nu_1}D_{\nu_1\nu_2}\cdots D_{\nu_j\nu_0}F^j\frac{1}{(\Delta_{\nu_1 0}-ij\gamma)\cdots(\Delta_{\nu_j 0}-i\gamma)}\right], \quad t\le 0 \tag{2.3a}$$

where the summations are performed over all sets $\nu_k=(n_k,l_k,m_k)$ of the spherical quantum numbers, including also the integration over the continuum energies, and

$$D_{\nu_i\nu_j}(t)=\langle\Phi_{\nu_i}|\mathbf{r}\cdot\hat{\mathbf{e}}|\Phi_{\nu_j}\rangle\ , \quad \Delta_{\nu_i\nu_j}=E_{n_i}-E_{n_j} \tag{2.3b}$$

and where indices ν_0 and 0 are equivalent. Restriction to negative time simplifies significantly the expression, due to specific nature of the time dependence of F in transition from $t<0$ to $t>0$, and it can be shown that extension of (2.3a) to $t>0$ would not influence our forthcoming conclusions.

By rearranging the terms in Eq. (2.3a) we obtain

$$\Psi=\Phi_0\exp(i\mathbf{g}\cdot\mathbf{r})+\sum_{j=1}^{\infty}\left[\sum_{\nu_1}\cdots\sum_{\nu_j}\Phi_{\nu_1}D_{\nu_1\nu_2}\cdots D_{\nu_j\nu_0}g^j\frac{i^j}{j!}S_j(\gamma)\right], \tag{2.4a}$$

where

$$S_j(\gamma)=\left[\frac{1}{(1+i\Delta_{\nu_1 0}/j\gamma)\cdots(1+i\Delta_{\nu_j 0}/\gamma)}-1\right] \tag{24.b}$$

and

$$g(t)=\int_{-\infty}^{t}F(t')dt'\ , \tag{2.4c}$$

with $\mathbf{g}=g(t)\hat{\mathbf{e}}$. Since $g\sim F_0/\gamma\equiv g_0$, the only field-dependent parameter that appears in Eq. (2.4a) is g_0.

Keeping g_0 finite but in the limit of infinitely short electric field pulse, we have $S_j(\gamma\to\infty)\to 0$, and therefore the first term in Eq. (2.4a) is the exact solution of the problem (2.1a) in this limit,

$$\Psi(t,\gamma\to\infty)=\Psi^{(0)}(t)=\exp(i\mathbf{g}\cdot\mathbf{r})\Phi_0(\mathbf{r},t)\ . \tag{2.5}$$

To determine the range of validity of approximation (2.5) for large but finite γ one should investigate the terms with $j\ge 1$ in the expansion (2.4). An additional time-dependent exponential factor could be extracted from the perturbation series, which significantly improves its convergence for large n. This is easily shown by making an ansatz on the exact wave function Ψ, in the form

$$\Psi=\exp\left[i\mathbf{g}\cdot\mathbf{r}-\int^{t}(g^2/2)dt'\right]\Psi_1\ , \tag{2.6}$$

which yields the Schrödinger equation for Ψ_1 with the new Hamiltonian

$$H_1=H_A-i\mathbf{g}\cdot\nabla\ . \tag{2.7}$$

The exact perturbation series for Ψ_1 can then be written in the form

$$\Psi_1=\Phi_0+\sum_{j=1}^{\infty}\left[\sum_{\nu_1}\cdots\sum_{\nu_j}\Phi_{\nu_1}D'_{\nu_1\nu_2}\cdots D'_{\nu_j\nu_0}g^j i^j\frac{1}{(\Delta_{\nu_1 0}-ij\gamma)\cdots(\Delta_{\nu_j 0}-i\gamma)}\right], \quad t\le 0\ , \tag{2.8a}$$

where

$$D'_{\nu_i\nu_j}(t)=\langle\Phi_{\nu_i}|\hat{\mathbf{e}}\cdot\nabla|\Phi_{\nu_j}\rangle\ . \tag{2.8b}$$

With the use of

$$D'_{\nu_i\nu_j}=\Delta_{\nu_j\nu_i}D_{\nu_i\nu_j} \tag{2.8c}$$

one can show that the successive terms in (2.8a) are of higher powers of parameter P_1, defined as

$$P_1=g_0\frac{s\langle r\rangle}{(1+s^2)^{1/2}}\ , \tag{2.9}$$

where $s=\Delta/\gamma$. If $s\ll 1$, which could always be achieved for given γ when the principal quantum number n is high enough, we have

$$P_1\to p'_1=h_0\frac{1}{n}\ , \tag{2.10}$$

where $h_0=g_0/\gamma$ and we used $\langle r\rangle\sim n^2$ and $\Delta\sim 1/n^3$. Therefore in the limit $1/\gamma n^3\ll 1$, the series in (2.8a) converges with $p'_1=h_0/n\ll 1$. Furthermore, rewriting P_1 as

$$P_1=\frac{g_0}{n}\left[\gamma^2+\frac{1}{n^6}\right]^{-1/2} \tag{2.11}$$

we can relax the condition $s\ll 1$ and conclude that

$$\Psi(t,n\to\infty)\to\Psi^{(0)} \tag{2.12}$$

always. We note that $\Psi^{(0)}(t)$ is the exact solution of the Schrödinger equation with the Hamiltonian

$$H'=H_A-\mathbf{F}\cdot\mathbf{r}+i\mathbf{g}\cdot\nabla\ . \tag{2.13}$$

In conclusion, the function

$$\Psi_1^{(0)}=\exp\left[i\mathbf{g}\cdot\mathbf{r}-i\int^{t}(g^2/2)dt'\right]\Phi_0 \tag{2.14}$$

tends to the exact solution of the Schrödinger equation (2.1) if one of the following conditions is fulfilled, and if g_0 is kept finite.

(a) Time duration of the electric field pulse is infinitely short, i.e., $\gamma\to\infty$. Then $P_1\to 0$ and $p'_1\to 0$.

(b) Principal quantum number n of Φ_0 tends to infinity. The fact that Φ_0 is coupled also to the states with smaller

n does not change this conclusion. We note that our estimate of the matrix element of $\mathbf{r}$ as proportional to its expectation value n_0^2 of the initial state could be relaxed somewhat for the off-diagonal element between the atomic states with $n \not\approx n'$. It decreases then with n as $(nn')^{-3/2}$. One of the consequences is that if $P_1 \leq 1$, the field-induced n mixing would decrease with increase of $|n-n_0|$, which is confirmed by exact numerical calculations in Sec. III.

(c) Hamiltonian H_A has only degenerate eigenstates, then $\Delta \to 0$ and $s \to 0$, resulting in $P_1 \to 0$.

In the previous derivation no reference has been given to the direction of the electric field, and it can be generalized to arbitrary instantaneous direction. Expanding $\exp(i\mathbf{g}\cdot\mathbf{r})$, and assuming Φ_0 a spherical state, Eq. (2.14) can be written in the form

$$\Psi_1^{(0)}(\mathbf{r},t)=4\pi\sum_l\sum_{m=-l}^{m=l} i^l j_l(gr)Y_{lm}(\vartheta,\varphi)Y_{lm}^*(\vartheta_g,\varphi_g) \times\Phi_0\exp\left[-i\int^t (g^2/2)dt'\right], \tag{2.15a}$$

where

$$g=[g_x^2(t)+g_y^2(t)+g_z^2(t)]^{1/2},$$
$$\vartheta_g(t)=\tan^{-1}(g_\rho/g_z),$$
$$\varphi_g(t)=\tan^{-1}(g_y/g_x),\quad g_\rho=(g_x^2+g_y^2)^{1/2}. \tag{2.15b}$$

This wave function contains all the hydrogenic components with various n,l,m, including continuum. Expanding it in unperturbed functions Φ_{nlm} as

$$\Psi=\sum_{n,l,m}\alpha_{nlm}\Phi_{nlm}$$

one obtains the amplitude for field-induced transitions in the form

$$\alpha_{\nu\lambda\mu}(t)=\exp\left[i(E_\nu-E_0)t-i\int(g^2/2)dt'\right](4\pi)^{1/2} \times\sum_l i^l\left[\frac{(2l_0+1)(2l+1)}{(2\lambda+1)}\right]^{1/2} \times\mathcal{R}(\nu\lambda,\ln_0 l_0)C(l_0 l\lambda,m_0 m\mu) \times C(l_0 l\lambda,000)Y_{lm}^*(\vartheta_g,\varphi_g), \tag{2.16a}$$

where

$$\mathcal{R}(\nu\lambda,lnl_0)=\int dr\, r^2 R_{\nu\lambda}j_l(gr)R_{n_0 l_0} \tag{2.16b}$$

is the radial matrix element of j_l, $m=\mu-m_0$, and

$$l=|\lambda-l_0|,|\lambda-l_0|+2,\ldots,\lambda+l_0.$$

The last formula is somewhat simplified if the electric field is in the direction of the z axis. In that case $\mu=m_0$, $\vartheta_g=0$, and $Y_{lm}^*(\vartheta_g,\varphi_g)\to[(2l+1)/4\pi]^{1/2}$.

The condition (b) has so far been studied only for bound states. The parameter of validity for the continuum states similar to the one in (2.11)–(2.13) may be obtained when $\Phi_0=\Phi_{E_k}$ where E_k is the kinetic energy of the unperturbed continuum. The energy-normalized continuum-continuum radial matrix element of r in region $\Delta E=E_k$, $-E_k \ll E_k$ is derived [21] which gives the largest contribution because of its singular nature,

$$R_l(E_k,E_k')\cong\frac{1}{2\pi}\left[\frac{2k}{(l^2k^2+1)^{1/2}(\Delta E)^2} +\frac{(l^2k^2+1)^{1/2}(l-1)}{2k\Delta E}\right], \tag{2.17}$$

where $k=\sqrt{2E_k}$. Replacing this in the first order of the expansion (2.8), the order of energy singularity in (2.17) is decreased by one (to $1/\Delta E$), and assuming $l=1$, one obtains

$$\Delta E R_1(E,E')=\frac{1}{\pi}\frac{k}{(k^2+1)^{1/2}\Delta E}, \tag{2.18}$$

which yields

$$\Psi^{(1)}=-\frac{gi}{\pi}\int dE\,\Phi_E\frac{k}{(k^2+1)^{1/2}\Delta E}\frac{1}{(\Delta E-i\gamma)}. \tag{2.19}$$

Using the formula

$$\frac{1}{\Delta E}=\mathcal{P}\frac{1}{\Delta E}\pm i\pi\delta(\Delta E), \tag{2.20}$$

where $\mathcal{P}$ is the principal value of the integral, and extending integration in ΔE to $(-\infty,\infty)$ in calculation of the principal value, we get for $\gamma \gg E_k$

$$P_{1k}=h_0\frac{2k}{(k^2+1)^{1/2}}. \tag{2.21}$$

In (2.21) the contribution from the pole $\Delta E=i\gamma$ is neglected, since the wave function Φ_E will exponentially fall off at large imaginary E. If $\gamma \ll E_k$, the expression similar to (2.21) is obtained. Therefore bounds of validity of (2.14) for dressing the continuum wave function $\Phi_k(t)$ by a time-dependent electric field are defined by smallness of the parameter

$$p_{1k}=h_0 k. \tag{2.22}$$

This is essentially the same condition as (2.10) for the bound states, with k replaced by $1/n$.

Ongoing calculation on dressing of hydrogenic continuum with time-dependent electric field by the use of Eq. (2.14) shows that only states within the continuum band $k-g_0<k'<k+g_0$ are strongly mixed in both k' and l. If $k<g_0$, bound states with $E_n \geq -(k-g_0)^2/2$ are also strongly mixed with the continuum. The calculation not only is formidable and time consuming but also contains problems intrinsic to the continuum mixing and will be published later in all its details.

A better insight into the two approximations is obtained by introducing a transformation on the wave function Ψ_1, as

$$\Psi_1=\exp(-\mathbf{h}\cdot\nabla)\Psi_2, \tag{2.23}$$

where $\mathbf{h}=\int\mathbf{g}(t)dt$. Then Ψ_2 satisfies the Schrödinger equation with the new Hamiltonian

$$H_2=-\frac{\Delta}{2}+V(\mathbf{r}+\mathbf{h}), \tag{2.24}$$

which describes the electron in a field of a nucleus, which moves classically with acceleration $\mathbf{F}(t)$; the action of the electric field on the electron is replaced by the accelerated center of force, where $\mathbf{r}$ is the electron position with respect to the nucleus which is moving. The approximation (2.14) results from approximating $\Psi_2(\mathbf{r},t)$ by $\Phi_0(\mathbf{r}+\mathbf{h}(t))$. The motion of the center of force is such that the electron adiabatically adapts to that motion. If $\Delta/\gamma<1$, this is fulfilled when the characteristic dimension of the electron orbit around the nucleus, v_A/γ, is much smaller than the wavelength $\lambda=1/g_0$ of the charge which is moving with velocity g_0. Therefore $(v_A/\gamma)/\lambda \ll 1$, i.e., $h_0/n \ll 1$, as was obtained earlier. It is to be noted that the larger rate of time change of the electric field yields the slower "motion" of the center of force, and "adiabaticity" of the nuclear motion is appropriate, as compared with the fast changing electric field. Furthermore, the formula (2.14) may be interpreted as a Galilean transformation from a coordinate system moving with velocity $\mathbf{g}$ to the laboratory system. It is well known [22] that sudden application of a magnetic field on an atomic system is equivalent to a rotation of the angular momentum of the system. We have here sudden application of an electric field to the system, which is equivalent to the translation of the center of force of the system.

To see if the transformation (2.23), together with approximation of the wave function $\Psi_2(t)$ by $\Phi_0(t)$, can bring improvement to (2.14) we note that such an approximation leads to the neglect of $\mathbf{h}$ in Hamiltonian (2.24), and anticipates that the important region of r is $r \gg h$. Using the exact perturbation series for Ψ_1, and rearranging the terms in (2.8) one can get

$$\Psi_1=\exp[-\mathbf{h}(t)\cdot\nabla]\Phi_0 + \sum_{n=1}^{\infty}\left[\sum_{\nu_1}\cdots\sum_{\nu_j}\Phi_{\nu_1}D'_{\nu_1\nu_2}\cdots D'_{\nu_j\nu_0} \times\frac{g^j(-1^j)}{\gamma^j j!}S_j(\gamma)\right], \quad t\le 0 , \tag{2.25}$$

where $S_j(\gamma)$ was defined in Eq. (2.4b). Since $S_j(\gamma\to\infty)=0$ if one keeps $h_0=g_0/\gamma$ finite in that limit, the zeroth-order term in (2.25a) is the exact wave function Ψ_1, i.e.,

$$\Psi_1(t,\gamma\to\infty)=\Psi_2^{(0)}(t)=\Phi_0(\mathbf{r}-\mathbf{h}(t),t) . \tag{2.26}$$

This yields a new approximation for the total wave function Ψ,

$$\Psi_I^{(1)}=\exp\left[i\mathbf{g}\cdot\mathbf{r}-i\int^t(g^2/2)dt'\right]\Phi_0(\mathbf{r}-\mathbf{h},t) , \tag{2.27}$$

which, unlike (2.14), approaches the exact wave function for $\gamma\to\infty$ but keeping h_0 finite, rather than g_0 in derivation of (2.14). Therefore (2.27) represents a quite different solution to the problem. It follows from the expansion (2.25a) that (2.14) is restored and a shift in Φ_0 is absent if all the eigenstates of Hamiltonian H_A are degenerate. To investigate the rate of convergence of (2.27) to the exact wave function with increasing principal quantum number n, we define the correction parameters from the expansion (2.25), assuming that $\Delta/\gamma \ll 1$. The first term gives $p^{(1)}=(h_0/\gamma)1/n^4$, the second term $p^{(2)}=(p^{(1)})^2\gamma n^3$ and $(p^{(1)})^2$, and the third term $p^{(3)}\sim p^{(1)3}(\gamma n^3)^2$, etc. Thus the fast convergence with n, shown with $p^{(1)}$, is lost in the higher-order terms of (2.25). Instead the series converges as $1/(\gamma n^3)[h_0/n+(h_0/n)^2+\cdots]$, if $\gamma n^3>1$. Therefore, although the correction terms are smaller in (2.25) by a factor Δ/γ than that in (2.16), the dependence on n is exactly the same in the two cases. In both cases we need the condition $h_0/n<1$ to be satisfied. In view of this conclusion, and having in mind numerical difficulties in evaluating (2.27) [in comparison to (2.14)], we do not further consider approximation (2.27).

A slightly different form of dressing from Eq. (2.5) is possible, where

$$\Psi(t,\gamma\to\infty)=\Psi^{(0)}(t)=\exp(-iH_At)\exp(i\mathbf{g}\cdot\mathbf{r}+iE_0t) \times\Phi_0(\mathbf{r},t) . \tag{2.28}$$

As will be discussed in the next section this form gives the same field-induced transition probabilities as Eq. (2.5) but provides better phase factors at the $t\to\infty$ limit, thus emphasizing the on-shell mixing of Φ_0.

B. "Long-pulse" approximation

In the case when $\Delta/\gamma \gg 1$, i.e., $\gamma n^3 \ll 1$, which is attainable when the time rate of the applied electric field is small in comparison to the characteristic period T of the atomic state, the approximations derived above could be applied if the principal quantum number of the states is not too high. In that case the approximation (2.14) is acceptable if

$$p_1''=g_0n^2\ll 1 , \tag{2.29}$$

which can be obtained from Eq. (2.11).

To consider the limit $\gamma\to 0$, keeping $g_0=F_0/\gamma$ finite, we will use the exact perturbation series (2.3a). If the states of H_A are nondegenerate, then we have $S_j(\gamma\to 0)=-1$ from (2.3b), and (2.3a) restores the unperturbed state $\Phi_0(t)$. Taking into account the degeneracy we set

$$S_j(\gamma\to 0)=\delta_{\nu_1 0}\delta_{\nu_2 0}\cdots\delta_{\nu_j 0}-1 , \tag{2.30}$$

where δ_{ij} stands for the Kronecker delta. Then (2.3a) becomes

$$\Psi=\Phi_0+\sum_{j=1}^{\infty}\left[\sum_{\nu_0'}\cdots\sum_{\nu_0(k)}\Phi_{\nu_0'}D_{\nu_0'\nu_0''}\cdots \times D_{\nu_0(k-1)\nu_0(k)}g^j\frac{i^j}{j!}\right], \tag{2.31}$$

where the summations are taken over all the states which are degenerate with $|0\rangle$. For the hydrogenic case, it is convenient to choose the basis functions Φ_{ν_0} in parabolic coordinates, in which case $D_{\nu_0\nu_0'}$ are diagonal [23,24],

$$D_{\nu_0\nu_0'}=\tfrac{3}{2}n(n_1-n_2)\delta_{\nu_0\nu_0'}=d_0(n_1,n)\ , \tag{2.32}$$

where n_1,n_2 are the parabolic quantum numbers, with $n_1+n_2+m+1=n$. Then (2.31) gives

$$\Psi(t)=\Phi_0^p(t)\exp[igd_0(n_1,n)]\ , \tag{2.33}$$

where Φ_0^p is the parabolic unperturbed wave function. If the unperturbed, initial wave function is a spherical state, then (2.33) can be used to construct the l-mixed state that evolves from $\Phi_{nl_0m_0}$. This yields [19]

$$\Psi=\sum_{n_1,n_2}\sum_{l}\langle nl_0m_0|n_1n_2m_0\rangle\langle n_1n_2m_0|nlm_0\rangle \times\exp[igd_0(n_1,n_2)]\Phi_{nlm_0}\ , \tag{2.34a}$$

where

$$\langle n_1n_2m|nlm\rangle=C((n-1)/2,(n-1)/2,l;(m+n_2-n_1)/2,(m+n_1-n_2)/2,m)(-1)^{\nu} \tag{2.34b}$$

and

$$\langle n_1n_2m|nlm\rangle=\langle nlm|n_1n_2m\rangle\ ,\quad \nu=n_2+(|m|-m)/2\ . \tag{2.34c}$$

$C(j_1,j_2,j_3;m_1,m_2,m_3)$ is the Clebsch-Gordan coefficient, in the notation of Rose [26]. The result is valid in the limit of $\gamma\to 0$ while keeping g_0 finite. For small but finite γ, mixing between nondegenerate states takes place and we estimate its contribution from the first-order term in (2.3a). This yields a small parameter of applicability for (2.34) in the form

$$P_2=F_0\langle r\rangle/(\gamma+\Delta)\ . \tag{2.35a}$$

If $\gamma n^3\ll 1$, we thus have

$$p_2''\cong F_0n^5 \tag{2.35b}$$

which is close to the Inglis-Teller [25] limit. (Strictly speaking, the Inglis-Teller limit is defined originally with $F_0n^5=\frac{1}{3}$ rather than with $F_0n^5=1$, as is used in this text.) But, for any given small γ, one can choose n large enough so that $\gamma n^3\gg 1$. In that case, from Eq. (2.35a)

$$p_2'\cong g_0n^2\ . \tag{2.35c}$$

It is interesting to note that the two approximations, (2.14) and (2.34) are of the same validity when $\gamma n^3\cong 1$. Then both P_1 in (2.11) and P_2 in (2.35a) are roughly equal to g_0n^2.

If the electric field is of arbitrary direction and the time dependences of the various components of the field differ from each other, the total field vector rotates. It is then not convenient to orient the fixed coordinate system in the direction of the field. The derivation leading to the formula (2.34) is still valid, however. One has to project the initial electric field vector onto the coordinate system that rotates with the parabolic coordinates, and projecting that solution to the spherical coordinates and then back to the fixed coordinate system we finally get

$$\Psi=\sum_{l,m}B_{lm}^{l_0m_0}\Phi_{nlm}\ , \tag{2.36a}$$

where the terms proportional to γ are neglected, and where

$$B_{lm}^{l_0m_0}(t)=\sum_{m'=-L}^{L}\sum_{n_1n_2}\langle nl_0m'|n_1n_2m'\rangle\langle n_1n_2m'|nlm'\rangle d_{m_0m'}^{l_0}(\vartheta(t))d_{mm'}^{l}(\vartheta(t)) \times\exp[i(m_0-m')\alpha(t)-i(m-m')\delta(t)+igd_0(n_1,n_2)]\ ,\quad L=\min(l,l_0)\ . \tag{2.36b}$$

The general form of the rotation operator R can be expressed in terms of the instantaneous Euler angles α,ϑ,δ of the field vector in the fixed coordinate system [26]

$$R=R(\alpha,\vartheta,\delta)=\exp(-i\alpha L_z-i\vartheta L_y-i\delta L_z)\ , \tag{2.37}$$

where $\mathbf{L}$ is the angular momentum operator. If the initially populated state is a spherical state, then in the rotated coordinate frame it contains a mixture of all m's, with the amplitudes determined by the matrix elements of

$$R(\alpha,\beta,\gamma)\phi_{nl_0m_0}=\sum_{m'}D_{m'm_0}^{l_0}(\alpha,\vartheta,\delta)\Phi_{nl_0m'}\ , \tag{2.38a}$$

where

$$D_{m'm}^{l}(\alpha,\vartheta,\delta)=\exp(im'\alpha-im\delta)d_{m'm}^{l}(\vartheta)\ , \tag{2.38b}$$

$$d_{m'm}^{l}(\vartheta)=\langle lm'|\exp(-i\vartheta L_y)|lm\rangle\ . \tag{2.38c}$$

The rotation matrix $d_{m'm}^{l}$ can be expressed in terms of Jacobi polynomials.

The approximate formula (2.14) has the form similar to the well known momentum-translation approximation (MTA) [27] in the theory of laser-atom interactions, where the role of $\mathbf{g}(t)$ is played by the laser field vector potential $\alpha_f\mathbf{A}(t)$, where α_f is the fine-structure constant. Although the formal difference between (2.14) and MTA is only in the sign of $\mathbf{g}$ (i.e., of $\alpha_f\mathbf{A}$ in the latter) in the exponent there is a more subtle difference. The MTA is derived as a low-frequency approximation for the laser-electron interaction defined in the $\mathbf{p}\cdot\mathbf{A}$ gauge [28], i.e., for the Hamiltonian similar to the one given in Eq. (2.7). The assumption

$$\tilde{\Psi}=\exp\left[-i\mathbf{g}\cdot\mathbf{r}-\int^{t}(g^2/2)dt'\right]\tilde{\Psi}' , \tag{2.39}$$

for the exact wave function $\tilde{\Psi}$ in the MTA case then yields $\tilde{\Psi}'$, which satisfies the Schrödinger equation with the Hamiltonian (2.1) ($\mathbf{r}\cdot\mathbf{E}$ gauge). Similarly as in derivation of parameter P_1 in (2.9), but with a different Hamiltonian, one obtains [22] the parameter $P'=P_2$, where P_2 was defined in Eq. (2.35a). The condition $P'\ll 1$ defines the range of validity of the MTA approximation, obtained by replacing Ψ' with Φ_0. This range completely overlaps with the one obtained for the "long-pulse" approximation (2.34a). The MTA and "short-pulse" approximation (2.14) represent solutions to different problems defined by the different Hamiltonians, and this explains almost disjoint bounds of their applicability, in spite of the formal similarity in expressions. This conclusion is not changed by the gauge invariance of the Hamiltonians (2.1) and (2.7) in the oscillating field case, since this invariance applies only to the exact wave functions. The forms (2.39) and (2.14) in the two gauges obviously give two different approximations.

III. NUMERICAL VERIFICATION

The approximations developed in Sec. II were tested by comparison with the exact numerical calculation involving a large, truncated set of bound states. The calculation was carried out by expanding the exact wave function of the problem, Eq. (2.1) in hydrogenic states $\Phi_\nu(t)$, where ν represent a set of spherical quantum numbers, as

$$\Psi=\sum_{\nu}\alpha_\nu(t)\Phi_\nu(t) . \tag{3.1}$$

Then, Eq. (2.1) yields a set of coupled differential equations for the amplitudes α_ν,

$$i\dot{\alpha}_\nu(t)=-\sum_{\nu'}\langle\nu|\mathbf{r}\cdot\mathbf{F}(t)|\nu'\rangle\alpha_{\nu'}(t)\exp(i\Delta_{\nu\nu'}t) . \tag{3.2}$$

Similarly, a set of coupled differential equations was solved for the amplitudes b_ν of the wave function Ψ_1, defined in Eqs. (2.6) and (2.7),

$$\dot{b}_\nu(t)=\sum_{\nu'}\langle\nu|\mathbf{r}\cdot\mathbf{g}(t)|\nu'\rangle\Delta_{\nu\nu'}b_{\nu'}(t)\exp(i\Delta_{\nu\nu'}t) , \tag{3.3}$$

where

$$\langle nlm|z|n'l'm'\rangle=\delta_{l',l\pm1}\delta m',m\times\left[\frac{l_>^2-m^2}{(2l_>+1)(2l_>-1)}\right]^{1/2}R_{n,l}^{n,l\pm1} , \tag{3.4a}$$

$$\langle nlm|x|n'l'm'\rangle=\delta_{l',l\pm1}\delta_{m',m\pm1}\frac{1}{2}\kappa\xi\times\left[\frac{(l_>+\xi+\kappa\xi m)(l_>+\kappa\xi m)}{(2l_>+1)(2l_>-1)}\right]\times R_{n,l}^{n,l\pm1} ,$$
$$\kappa=\mathrm{sgn}(m'-m) , \quad \xi=\mathrm{sgn}(l'-l) . \tag{3.4b}$$

$R_{n,l}^{n,l\pm1}$ are radial matrix elements of r, expressible analytically in terms of terminating hypergeometric functions.

Throughout the calculations of this section exponential time dependence of the field was assumed, and the field vector was chosen to lie in the plane $y=0$, i.e.,

$$\mathbf{F}(t)=F_{0z}\exp(-\gamma_z|t|)\hat{\mathbf{z}}+F_{0x}\exp(-\gamma_x|t|)\hat{\mathbf{x}} , \tag{3.5a}$$

with two time constants, γ_z and γ_x. We assume that the different components of F_0 and γ's are of the same order of magnitude. In that case time-dependent angles ϑ_g and φ_g that appear in Eq. (2.16) are

$$\vartheta_g=\tan^{-1}\left[\frac{F_{0x}\gamma_z}{F_{0z}\gamma_x}\right]\exp(-\Delta\gamma|t|)\times\begin{cases}1, & t\le 0\\ \dfrac{2\exp(\Delta\gamma t)-1}{2\exp(-\Delta\gamma t)-1}, & t>0\end{cases} ,$$
$$\Delta\gamma=\gamma_x-\gamma_z , \quad \varphi_g=0 . \tag{3.5b}$$

When the time constants of both components are the same, i.e., $\Delta\gamma=0$, ϑ_g becomes constant. The field, as given by Eq. (3.5a), mixes all states in m, l, and n. If one aligns the z axis in the direction of constant ϑ_g, only (n,l) mixing is present.

On the other hand, when the conditions for applicability of approximation (2.36) are met, only the Euler angle $\vartheta-\vartheta_g$ is needed for rotation of the coordinate system ($\alpha=\delta=0$) and therefore

$$D^l_{m'm}(0,\vartheta,0)=d^l_{m'm}(\vartheta_g) . \tag{3.6}$$

We calculate the rotation matrix from the expression [29]

$$d^l_{m'm}(\vartheta)=\left[\frac{(l-m')!(l+m')!}{(l+m)!(l-m)!}\right][\cos(\vartheta/2)]^{\nu}\times[\sin(\vartheta/2)]^{\mu}P^{\mu,\nu}_{l-m}(\cos\vartheta) ,$$
$$\nu=m'+m , \quad \mu=m'-m , \quad m'\ge m , \tag{3.7a}$$

with the addition of the symmetry property

$$d^l_{m'm}(\vartheta)=(-1)^{m'-m}d^l_{mm'}(\vartheta) . \tag{3.7b}$$

$P_j^{(\nu,\mu)}(x)$ is the Jacobi polynomial.

Equations (3.2) and (3.3) were solved in the truncated bases of the bound states. In the case of a one-component field directed along the z axis, the states up to $n=30$ were included in the basis. The actual number N of equations coupled depends on the chosen magnetic quantum number. For $m=0$, $N=465$ which implied solving of 930 coupled equations for the amplitudes. In the case of a two-component field, all states up to $n=10$ were included (385); that is, 770 coupled equations were solved, for different values of γ's and F_0.

In order to test the proposed approximations (2.5), (2.14), (2.27) and (2.33), (2.34), (2.36), sets of coupled equations (3.2) are solved for 70 cases by varying the initial state, the field amplitude, and γ (49 cases for the one-component field and 21 for the two-component field).

In addition, the coupled equations (3.3) are solved for 27 samples of parameters. These "exact" results were then used to compare the predictions of the approximate formulas. The general conclusion of the extensive study is that the approximations, in spite of their simplicity, agree surprisingly well in all details with the exact values, so long as the parameters are within the limits shown in Fig. 1. Comparison is done for the amplitudes that describe the n, l, and m mixing caused by the field.

A. One-component field

1. n mixing

The formula (2.14) in its expanded form (2.15), describes the n mixing caused by the field, with an overall relative error of less than parameter P_1, defined by (2.11). This is confirmed by comparison of the squares of amplitudes (2.16), with the exact solution. The total n mixing from initial state (n_0,l_0,m_0) is defined as the probability that the electrons leave the manifold of states (n_0). The probabilities are obtained from formula (2.14) for $F_0/\gamma=g_0=0.03$, and $\gamma t=10$. The horizontal lines in Fig. 3 represent the given parameters, with doubled value of the field amplitude. The reason for doubling comes from the fact that for large $t>0$ ($\gamma t\gg 1$), g tends to the value $2F_0/\gamma$, which has the same effect as having $2F_0$ at $t=0$, where parameter P_1, Eq. (2.11), was defined. The exact calculation shows the scaling with g_0, as γ is varied. The initial states chosen for Fig. 2 are for $l_0=m_0=0$. In the upper curve, both Inglis-Teller and long-pulse limits are crossed between $n=4$ and 5, which results in an abrupt increase of the n mixing. Although $P_1\simeq 1$ for $5<n<10$, the departure of the probabilities from the exact values stays at less than 50%, and decreases to a few percent for $n>15$, showing further improvement with increasing n. The lower curve in Fig. 2 corresponds to the lower horizontal line in Fig. 3, and stays well below the short-pulse line for all times, implying better agreement with the exact data. Besides, it crosses the long-pulse limit at $n=13$, and therefore the n mixing rises above 10% for $n\geq 13$.

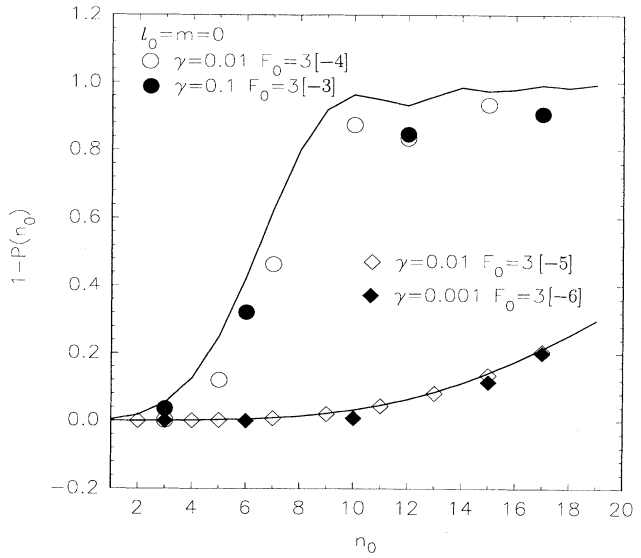

FIG. 2. Total field-induced n mixing as a function of the initial state principal quantum number n_0, at $\gamma t=10$. Solid lines are the "short-pulse" approximation (2.14), for $\gamma=0.01$ and $F_0=3\times 10^{-4}$ a.u. (upper line) and $F_0=3\times 10^{-5}$ (lower line); symbols represent the exact result, for various values of γ and F_0. The numbers in square brackets denote powers of 10.

The individual n mixing probabilities are shown in Fig. 4, for $\gamma=0.01$, $t=0$, and varying the field amplitude F_0. Initially, the atom is in $(n_0=10,l_0=1,m=0)$. The parameter values of the tested cases for Fig. 4 are shown

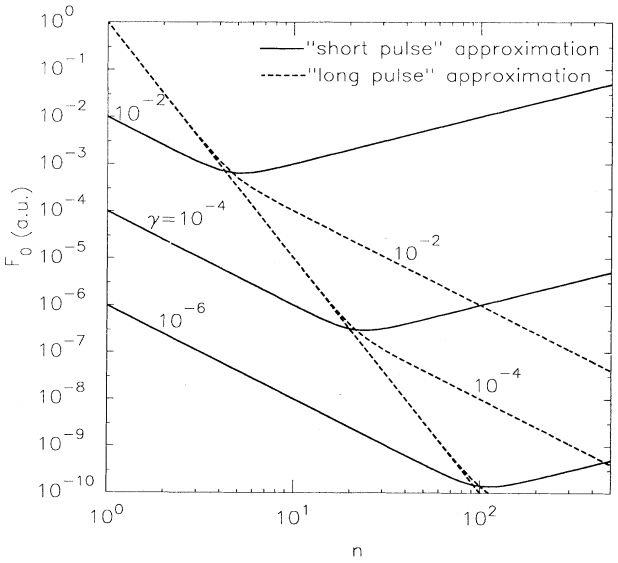

FIG. 1. Bounds of validity of the field-dressed bound states derived under the conditions that parameters $p_1=1$ (solid lines) and $p_2=1$ (dashed lines). The valid (F_0,n) regions with γ fixed are below the curves.

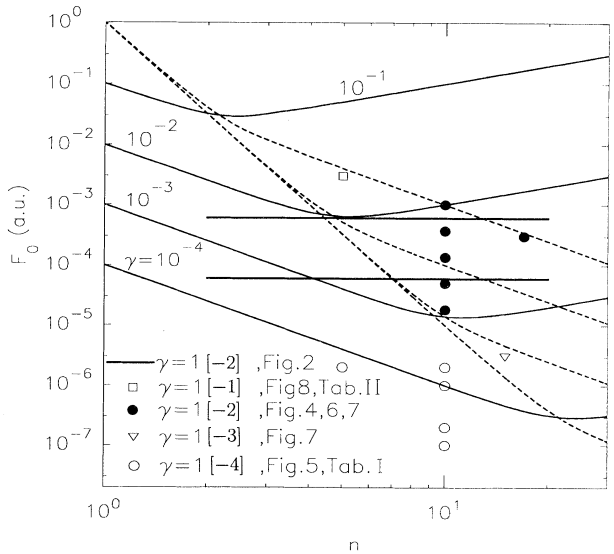

FIG. 3. Position of the test values of γ, F, and n of Figs. 2–8 and Tables I and II in the (F,n) diagram of Fig. 1. Horizontal lines represent the test values of Fig. 1 at $\gamma t=10$.

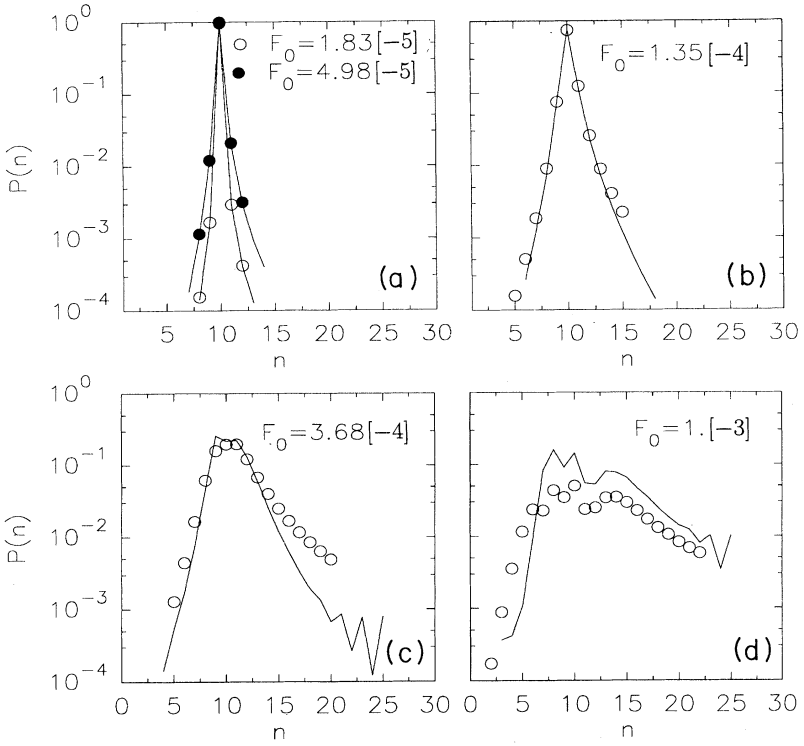

FIG. 4. Field-induced n mixing of the states, starting from the state $n_0=10$, $l_0=1$, and $m_0=0$, with $\gamma=0.01$ and for various values of the electric field amplitude F_0. Solid lines represent the exact values; symbols are the values obtained from "short-pulse" approximation (2.14).

with black dots in Fig. 3. All the tested cases were above the Inglis-Teller limit, but the n mixing still stays under 10% for the values below the long-pulse limit, as shown by the sharply peaked curves in Fig. 4(a). Upon crossing the long-pulse limit [Fig. 4(b)] the n mixing increases abruptly, but the approximation (2.14) reproduces the exact values. Even if P_1 is as big as $\frac{1}{2}$ [Fig 4(c)], the dominant part of the curve is reproduced within 5%. At crossing of the short-pulse limit [$P_1=1$, Fig. 4(d)], where the mixing tends to be more uniform in n, the distribution of the approximate transition probabilities reproduces qualitatively the exact distribution, although quantitative disagreement of the two curves reaches 50% at peak values

2. *l mixing*

When the l mixing is small and the field strength is below the Inglis-Teller limit, both the long-pulse approximation (2.34) and the short-pulse approximation (2.14) describe the l mixing almost exactly. In Fig. 5(a) the two approximations and the exact results are shown to almost coincide with each other for the lowest-field values in Fig. 3 (hollow circles) and for the initial state (10,1,0) at $t=0$ and for $\gamma=10^{-4}$. An interesting case is the curve for $F_0=10^{-6}$ in Fig. 5(a), where the field parameters reach the short-pulse limit, while being still below the Inglis-Teller limit. Then, the long-pulse approximation agrees well with the exact results, while the short-pulse approximation (2.14) starts to deviate, showing a spurious n mixing. This effect is even more pronounced at $\gamma t=10$ (dotted circles in Fig. 3), where the higher-field curve shows the spurious n mixing of the short-pulse approximation as much as 20%, resulting in errors in the l-mixing prob-

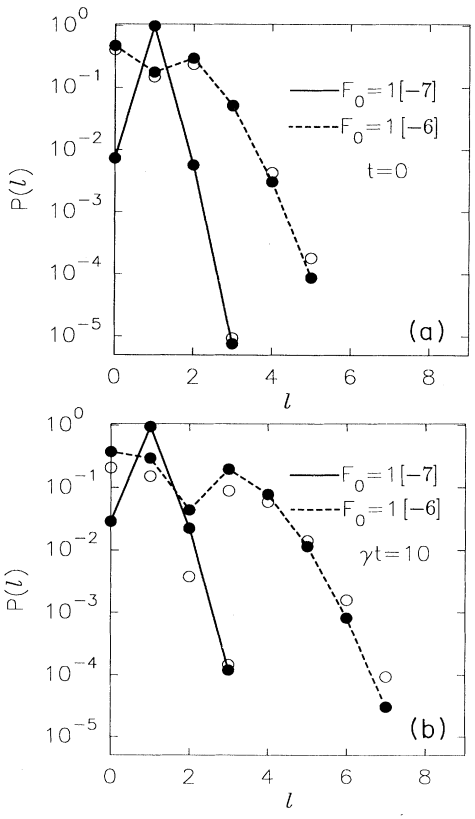

FIG. 5. Field-induced l mixing within the initial $n_0=10$ manifold of states ($l_0=1$, $m_0=0$), with $\gamma=1\times10^{-4}$, at $\gamma t=0$ (a) and $\gamma t=10$ (b). The exact values are presented by solid and dashed lines; "long-pulse" approximation: filled circles; "short-pulse" approximation: hollow circles.

abilities. Figure 6 shows the l-mixing probabilities where the n mixing is present, corresponding to the cases studied in Figs. 4(a)–4(c). The long-pulse approximation overestimates the transition probabilities (black circles), although they qualitatively follow the shape of the exact curves. On the other hand, the short-pulse approximation also gives correct substructure of the l-mixing probabilities (in the parameter region where it correctly describes the n mixing). Figure 6(c) is an exception. Fig. 4(c) shows that at $n=10$, the sharp peak of the n-mixing distribution is not reproduced by Eq. (2.16), introducing an error of about 20% for that particular value of $n \simeq 10$. This discrepancy is also visible in the l distribution in Fig. 3(c). But the l distribution of probability in the other $n \neq n_0$ channels is quite correct, as can be seen in Fig. 6(d), for the transitions $(10,1,0) \rightarrow (12,l,0)$.

3. *The time development of the system*

Although we compared the distributions generated in the approximation (2.14) and (2.34) with the exact results at typical times $t=0$ and ∞, the approximations follow in all details the exact evolution in time as long as we stay within the range of validity as described in Figs. 1 and 3. As was noted earlier, this range is determined essentially by the scaling of the response of the system by $g=\int F(t)dt$. If the scaling is maintained for the $g=2F_0/\gamma=g(+\infty)$, the approximations remain valid for all times, each within its range. Figure 7(a) represents the comparison of the short-pulse approximation and the exact probabilities in the elastic channel (n_0,l_0,m_0), where the initial states are (15,4,2) and (17,0,0). The position of the test cases in the (F,n) diagram of Fig. 3 corresponds to the time $t=0$, and obviously stays below (although approaching closely) the short-pulse limit when $t \rightarrow \infty$. In both cases, (2.14) reproduces the exact curves. The same is valid for the evolution of the total n mixing from the initial state (15,4,2), as well as for the l mixing, presented in Fig. 7(b).

Our numerical investigation indicates that at $\gamma t \gg 1$, the dressed wave function in Eq. (2.28) provides better oscillating phase factors for each mixed component in Ψ than the one in Eq. (2.5). This suggests that for the $t \sim 0$, where $|\gamma t| < 1$, both forms are acceptable. On the other hand, Eq. (2.5) is much easier to use in the evaluation of the collisional and radiative transition amplitudes that involve dressed states Ψ. This is especially true for the dressing of continuum states.

B. Two-component electric field

In order to test formulas (2.16) and (2.36) for $\theta_g \neq 0$, we assume that the electric field can be represented by two components, along the z and x axes, which develop in time with two arbitrary time constants. The resultant field rotates in the plane $y=0$, and the m mixing of the states becomes important. This significantly increases the number of simultaneously coupled states, and restricts the largest n manifold that can be treated numerically. We restrict the set in (3.1) and (3.2) to the manifolds of

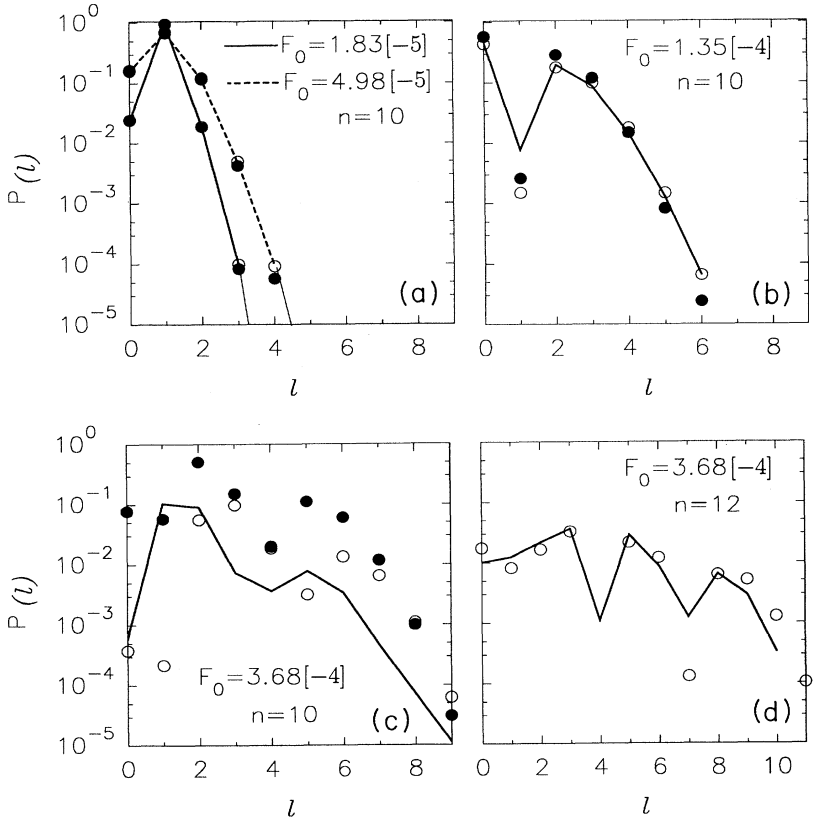

FIG. 6. Field-induced l mixing, within the initial $n_0=10$ manifold of states ($l_0=1$, $m_0=0$: (a)–(c), and within $n=12$ manifold of states, (d), with $\gamma=0.01$, at $\gamma t=0$. Lines represent the exact probabilities, and meaning of the symbols is as in Fig. 5.

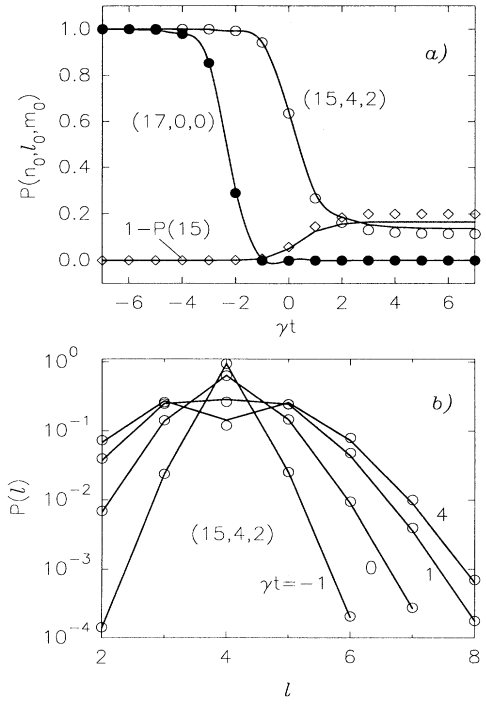

FIG. 7. The time evolution of the probabilities of "short-pulse" approximation (symbols) vs the exact values (lines). (a) Hollow circles; $n_0=15$, $l_0=4$, $m_0=2$; values represent the probabilities of staying in the initial state when $\gamma=10^{-3}$, $F_0=3\times10^{-6}$; filled circles: $n_0=17$, $l_0=0$, $m_0=0$, at $\gamma=0.01$ and $F_0=3\times10^{-3}$, and the meaning of the values is the same as the first case, hollow squares: The validity conditions are the same as in the first case but the values represent the total probability of leaving the initial $n_0=15$ manifold of states. (b) The l-mixing probabilities within initial manifold of states for different times, with $n_0=15$, $l_0=1$, $m_0=0$, $\gamma=10^{-3}$, $F_0=3\times10^{-6}$.

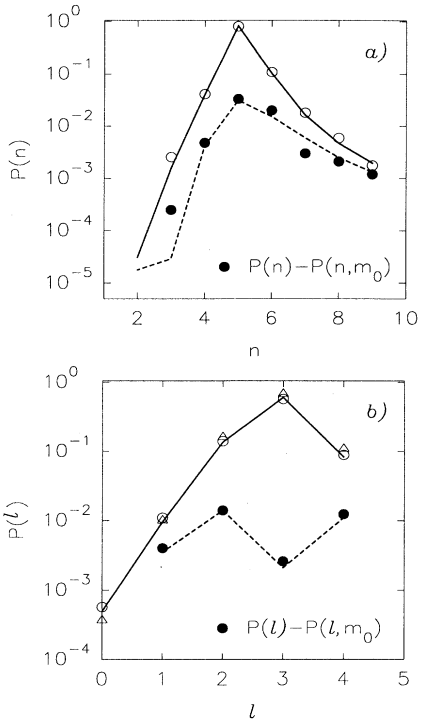

FIG. 8. The (a) n- and (b) l-mixing probabilities of the states in the presence of m mixing, starting from the state with $n_0=5$, $l_0=3$, $m_0=1$. The hollow circles represent the "short-pulse" approximation, hollow triangles are the exact values. The filled circles are the corresponding total m-mixing probabilities. $F_{0x}=F_{0z}=3\times10^{-3}$, $\gamma_x=2\gamma_z=0.2$.

states up to $n=10$, choosing the two components of the field amplitudes equal, $F_{0z}=F_{0x}$, but with the time constants γ different by a factor of 2, as $\gamma_x=2\gamma_z$, i.e.,

$$F_x=F_0 f(t)\exp(-2\gamma|t|)\ ,\quad F_z=F_0\exp(-\gamma|t|)\ ,$$

where $f(t)$ is a slowly varying function of t.

Table I summarizes the detailed transition amplitudes from the initial state (5,3,1), with $f(t)=1$, $\gamma t=10$, $\gamma=10^{-4}$, and $F_0=10^{-6}$. Only amplitudes whose dominant part is larger than 0.01 are presented. These parameters, as seen in Fig. 3, lie well below the Inglis-Teller limit, and also below but close to the short-pulse limit. The long-pulse formula (2.36) in all details reproduces the exact results to three significant digits. The short-pulse formula (2.16) also works well for these parameters, al-

TABLE I. The amplitudes obtained by the exact calculation, by the "long-pulse" and by the "short-pulse" approximation, with $n_0=5$, $l_0=3$, $m_0=1$, $\gamma_x=2\gamma_z=2\times10^{-4}$, $F_{0x}=F_{0z}=10^{-6}$. Only the dominant transitions are shown. No n mixing was present. $a[b]=a\times10^{-b}$.

5,3,1	Exact		LP		SP	
↓	Reα	Imα	Reα	Imα	Reα	Imα
(5,1,0)	−2.97[2]	4.03[6]	−2.96[2]	0.00	−3.16[2]	0.00
(5,1,1)	−3.74[2]	1.38[6]	−3.74[2]	0.00	−4.02[2]	0.00
(5,2,0)	−2.52[5]	8.22[2]	0.00	8.21[2]	0.00	7.78[2]
(5,2,1)	−6.52[5]	2.74[1]	0.00	2.74[1]	0.00	2.64[1]
(5,2,2)	7.01[7]	−3.80[2]	0.00	−3.80[2]	0.00	−3.85[2]
(5,3,1)	9.27[1]	2.32[4]	9.27[1]	0.00	8.85[1]	0.00
(5,3,2)	−1.54[2]	2.63[5]	−1.54[2]	0.00	2.20[2]	0.00
(5,4,0)	1.32[5]	−4.83[2]	0.00	−4.82[2]	0.00	−4.62[2]
(5,4,1)	−6.50[5]	2.14[1]	0.00	2.14[1]	0.00	2.04[1]
(5,4,2)	−3.01[5]	7.47[2]	0.00	7.47[2]	0.00	6.97[2]

TABLE II. The m-mixing amplitudes in the presence of n mixing, under the conditions of Fig. 8. $a[b]=a\times10^{-b}$.

(5,3,1)	Exact		LP		SP	
↓	Reα	Imα	Reα	Imα	Reα	Imα
(4,1,0)	3.47[2]	4.22[3]			3.55[2]	0.00
(4,1,1)	−4.51[2]	−5.45[3]			−4.58[2]	0.00
(4,2,0)	5.56[3]	−4.55[2]			0.00	−5.11[2]
(4,2,1)	−1.97[2]	1.59[1]			0.00	1.77[1]
(4,3,1)	−8.83[2]	−8.68[3]			−5.23[2]	0.00
(5,1,0)	5.88[2]	4.71[4]	6.26[2]	0.00	6.30[2]	0.00
(5,1,1)	−7.81[2]	−6.64[4]	−8.09[2]	0.00	−8.35[2]	0.00
(5,2,0)	2.00[4]	−9.85[2]	0.00	−1.13[1]	0.00	−9.98[2]
(5,2,1)	−9.46[4]	3.49[1]	0.00	3.89[1]	0.00	3.55[1]
(5,2,2)	−3.93[4]	6.13[2]	0.00	6.06[2]	0.00	6.22[2]
(5,3,1)	7.74[1]	−1.13[4]	8.40[1]	0.00	7.55[1]	0.00
(5,3,2)	4.00[2]	4.42[4]	3.31[2]	0.00	4.51[2]	0.00
(5,4,0)	−3.16[4]	6.17[2]	0.00	7.08[2]	0.00	6.43[2]
(5,4,1)	−1.10[3]	2.68[1]	0.00	3.12[1]	0.00	2.77[1]
(5,4,2)	3.24[4]	−8.65[2]	0.00	−1.07[1]	0.00	−9.08[2]
(6,3,1)	−1.76[1]	1.06[2]			−1.24[1]	0.00
(6,4,0)	2.82[3]	5.13[2]			0.00	5.94[2]
(6,4,1)	1.14[2]	2.15[1]			0.00	2.51[1]
(6,4,2)	−3.45[3]	−6.18[2]			0.00	−7.80[2]
(6,5,0)	−4.99[2]	2.65[3]			−5.39[2]	0.00
(6,5,1)	−9.58[2]	5.06[3]			−1.02[1]	0.00
(6,5,2)	6.90[2]	−3.64[3]			7.53[2]	0.00

though it gives the spurious n mixing of about 4% that is reflected in the results.

An interesting test of the present approximations is the case when one of the electric field components (F_x) is an odd function of time. Then $g_x=\int_{-\infty}^{t}F_x(t')dt'$ vanishes at $t\to+\infty$, and the m mixing is expected to vanish in the same limit. This is indeed the case. Assuming $f(t)=2\gamma t$, $\gamma=0.1$, $F_0=3\times10^{-3}$, the exact calculation with (5,3,1) initial state shows that the m-mixed amplitudes are less than one order of magnitude of the corresponding l-mixed amplitudes. This is not true at smaller t. The transition amplitudes to the different (n,l,m) states, whose magnitudes are larger than 0.001 at $t=0$, are presented in Table II. For this set of parameters, the n mixing is found to be about 17%, but this is not given by the long-pulse approximation. The short-pulse formula (2.17) describes quite accurately both the n and l mixing (in the presence of the m mixing), as shown in Fig. 8, and much better than the long-pulse approximation. Finally, in Fig. 8, the total m mixing for the various n and l is presented and compared with the exact results, showing excellent agreement.

IV. CONCLUSIONS

The field-dressed atomic functions (2.14) and (2.34) accurately describe, each within their bounds of validity, all details of the field effect on the atomic system, incorporating the m, l, and in the case of (2.14), n mixing of the states. There are three validity regions in the parameter space of (F_0,γ,n) which are bounded by the Inglis-Teller (IT), "long-pulse" (LP), and "short-pulse" (SP) limits. They are defined in terms of the field amplitude F_0, its time constant $1/\gamma$, and the principal quantum number n of the initial atomic states. For the field parameters that are simultaneously below the IT and SP limits in the (F_0,n) diagram of Fig. 1, both (2.14) and (2.34) are valid, describing the situation with negligible n mixing. If the SP limit is below the IT limit in this region, (2.34) describes better the (l,m) mixing, since (2.14) can show a small spurious n mixing. Between the IT and LP limits, the n mixing is less than 10%, and again both (2.14) and (2.34) can be used, although (2.14) describes more correctly the small n mixing and therefore the corresponding l and m mixing of the states. But above the LP limit the n mixing becomes strong, and can reach 95% as one approaches the SP limit from below. In that region only (2.14) can be used successfully; the result is better with higher n. This is a consequence of the n dependence of the SP limit, described by P_1 in (2.11) which is inversely proportional to n. For given field parameters, the farther the SP limit lies higher in the (F_0,n) plane of Fig. 1, the more accurate is the dressing described by (2.14). This is especially important for HRS; it was shown in Sec. II that (2.14) tends to the exact solution (for given γ and F_0) when $n\to\infty$. In addition, (2.14) is an exact solution for any n if the field duration tends to 0 ($\gamma\to\infty$), while keeping F_0/γ finite. We also note that (2.14) coincides with (2.34) if the Hamiltonian is infinitely degenerate, and this fact is responsible for the overlap of the bounds of validity for (2.14) and (2.34) in some range of the field and atomic system parameters. On the other hand, (2.34) tends to the exact solution of the problem if the field duration is infinitely long ($\gamma\to0$), while keeping F_0/γ finite, that is, for very small F_0.

In the case of PFE's with a dipole perturber field (1.1),

one can adopt these conclusions for slightly modified plasma parameters. First of all, as discussed in the Introduction, the exponential time dependence studied here is not an essential limitation. We showed [20] by comparison with the exact test calculations that conclusions similar to those presented here may be obtained for different time dependences, if F_0 and γ are defined properly. In the case of the dipole perturber, proper choice is $\gamma = v/b$ and $F_0 = 1/b^2$. Then p_1' in (2.10) becomes $p_1' = 1/(v^2 n)$, and obviously, for the electron plasma perturbers with $v \geq 1$ a.u., (2.14) is an acceptable approximation for all n. For the HRS, the electron temperature ($\sim v^2$) could be substantially reduced and still meet the validity criteria. On the other hand, for the ion plasma perturbers, their temperature must be above M (ionic mass in a.u.), or n is extremely high for (2.14) to be valid. In that case the IT limit defined by $p_2'' = n^5/b^2$, and the LP limit, $p_2' = n^2/vb$, may be appropriate, especially for the most important region, $n \leq 50$, keeping in mind that the dipole perturber approximation assumes $b \gg n^2$. (This imposes limitations on the applied plasma density.) These problems will be investigated in detail in forthcoming publications [8,20].

We finally note that, although the numerical check of the field-dressed wave functions has been done on atomic hydrogen, the result presented here can be applied to a more complex atom, with one or more active electrons. This investigation is in progress.

ACKNOWLEDGMENTS

This work was supported in part by DOE Grant No. FE-FG02-91ER14216, Fundamental Interactions Branch, Division of Chemical Sciences, and by a University of Connecticut Research Foundation Grant.

[1] M. J. Seaton, Adv. At. Mol. Phys. **11**, 83 (1975).
[2] A. Muller, in *Physics of Electronic and Atomic Collisions,* edited by A. Dalgarno *et al.,* AIP Conf. Proc. No. 205 (AIP, New York, 1990), p. 418.
[3] Y. Hahn, Adv. At. Mol. Phys. **21**, 123 (1985).
[4] D. S. Belić *et al.,* Phys. Rev. Lett. **50**, 339 (1983); A. Muller *et al., ibid.* **56**, 127 (1986).
[5] K. LaGattuta and Y. Hahn, Phys. Rev. Lett. **51**, 5581 (1983); V. Jacobs *et al., ibid.* **37**, 1390 (1976).
[6] G. Peach, Adv. Phys. **30**, 367 (1981).
[7] M. Baranger, Phys. Rev. **111**, 481 (1958); in At. Mol. Phys., edited by D. R. Bates (Academic, New York, 1962), Chap. 13.
[8] Y. Hahn and P. Krstić, Phys. Scr. **48**, 340 (1993).
[9] H. R. Griem, *Plasma Spectroscopy* (McGraw-Hill, New York, 1964); *Spectral Line Broadening by Plasmas* (Academic, New York, 1974).
[10] A. C. Kolb and H. R. Griem, Phys. Rev. **111**, 514 (1958).
[11] D. R. Bates, A. E. Kingston, and R. W. P. McWhirter, Proc. R. Soc. London, Ser. A **267**, 297 (1962).
[12] A. Burges and H. Summers, Astrophys. J. **157**, 1007 (1969).
[13] D. V. Fursa and G. L. Yudin, Phys. Rev. A **44**, 7414 (1991).
[14] D. A. Harmin, Phys. Rev. A **44**, 433 (1991).
[15] R. Damburg, in *Atoms in Strong Fields,* Vol. 212 of *NATO Advanced Study Institute, Series B: Physics,* edited by C. A. Nicolaides *et al.* (Plenum, New York, 1990), p. 107.
[16] D. A. Harmin, in Ref. [15], p. 61.
[17] D. Kondratovich and V. Ostrovsky, Zh. Eksp. Teor. Fiz. **83**, 1256 (1982) [Sov. Phys. JETP **56**, 719 (1982)].
[18] D. A. Harmin, Phys. Rev. A **24**, 2491 (1981); Phys. Rev. Lett. **49**, 128 (1982); Phys. Rev. A **26**, 2656 (1982).
[19] P. Krstić and Y. Hahn, J. Phys. B **26**, L291 (1993).
[20] P. Krstić and Y. Hahn (unpublished).
[21] F. Trombetta, S. Basile, and G. Ferrante, J. Opt. Soc. Am. B **7**, 598 (1990).
[22] E. Majorana, Nuovo Cimento **9**, 43 (1932).
[23] U. Fano, Phys. Rev. A **24**, 619 (1981).
[24] L. Pan, B. Sundaram, and L. Armstrong, J. Opt. Soc. Am. B **4**, 754 (1987).
[25] D. R. Inglis and E. Teller, Astrophys. J. **90**, 439 (1939).
[26] M. E. Rose, *Elementary Theory of Angular Momentum* (Wiley, New York, 1961).
[27] H. R. Reiss, Phys. Rev. A **1**, 803 (1970); **39**, 2449 (1989).
[28] M. H. Mittleman, *Introduction to the Theory of Laser-Atom Interactions* (Plenum, New York, 1982).
[29] A. R. Edmonds, *Angular Momentum in Quantum Mechanics* (Princeton University Press, Princeton, NJ, 1957).